Nonlocal Complex Ginzburg-Landau Equation for Electrochemical Systems

Vladimir García-Morales* and Katharina Krischer†
Physik-Department E19, Technische Universität München, James-Franck-Str. 1, D-85748 Garching, Germany

(Received 13 September 2007; published 6 February 2008)

By means of an extended center-manifold reduction, we derive the nonlocal complex Ginzburg-Landau equation (NCGLE) valid for electrochemical systems with migration coupling. We carry out the stability analysis of the uniform oscillation, elucidating the role of the nonlocal coupling in electrochemical systems at the vicinity of a supercritical Hopf bifurcation. We apply the NCGLE to an experimental system, an N-type negative differential resistance electrochemical oscillator, which is shown to exhibit electrochemical turbulence for wide parameter ranges.

DOI: 10.1103/PhysRevLett.100.054101 PACS numbers: 05.45.−a, 47.54.−r, 82.40.Bj

The dynamics of coupled oscillatory systems is of great relevance to physics, chemistry, and biology [1]. The coupling of an ensemble of oscillators can be local, global, or intermediate, depending on its spatial extension. In the vicinity of a supercritical Hopf bifurcation (SHB), local coupling can be most generally described in terms of the complex Ginzburg-Landau equation (CGLE). Consequently, much effort has been devoted to the study of the CGLE in the last two decades [1,2]. The understanding of intermediate and global coupling [we shall call it here *nonlocal* coupling (NLC)] remains however at its infancy. Kuramoto [3] formulated a nonlocal CGLE for a class of three (or more) component reaction-diffusion systems that, although having partial similarity with some chemical oscillators with coupling mediated by diffusive chemicals, is not directly related to any experimental system [4]. This equation predicts novel dynamical states, such as multiaffine turbulence [5] and chimera states [6].

NLC occurs naturally in electrochemical systems [7]. Here, the electrostatic potential at the working electrode (WE) is a dynamical variable, and any deviation from its average value decays with $\sim 1/r$ where r is the distance to a reference position. Thus, an inhomogeneity is felt instantaneously by a neighboring *range* of locations. This effect is called migration coupling and is synchronizing, smoothing out any potential gradients tangential to the WE in the absence of nonlinear reactions [7]. It can drive the system to turbulent states even without any diffusing species, as also found experimentally [8]. A further peculiar property of migration coupling is that the coupling range can be easily controlled by varying the distance w between the WE and the counter electrode (CE). The coupling range is determined by the aspect ratio $\beta \equiv w/L$, where L is the length of the WE [8,9]. For $\beta \to 0$, the local coupling limit is approached and the dynamics can be approximated by the CGLE. However, for finite, i.e., realistic β, the spatial coupling is nonlocal, and the CGLE cannot be applied.

In this Letter, we derive the nonlocal CGLE (NCGLE) valid for a wide class of electrochemical systems of experimental interest. This is achieved rigorously by means of an extended center-manifold reduction of the dynamics close to a SHB. Compared to recent related work [1,3,4], our derivation deviates substantially in the way the spatial scaling enters. We take explicitly into account the nonlocal kernel of the inhomogeneous dynamics in electrochemical systems [10]. The resulting NCGLE depends on only one additional parameter, the coupling range β (that fully controls the nonlocal kernel, in contrast to [4]) and reduces to the CGLE for $\beta \to 0$. Although the NCGLE can be extended to some 2D electrodes, we focus our attention to 1D ring electrodes because of their enormous experimental interest [7–12]. Our starting point is the dynamics for the double layer potential ϕ_{DL} coupled to the homogeneous reaction kinetics governing the evolution of a vector of chemical species $\mathbf{c}$ [8]

$$\partial_t \phi_{\mathrm{DL}} = f(\phi_{\mathrm{DL}}, \mathbf{c}) - \frac{\sigma}{\beta}(\partial_z \phi + \phi)|_{z=\mathrm{WE}} \tag{1}$$

$$\partial_t \mathbf{c} = \mathbf{g}(\phi_{\mathrm{DL}}, \mathbf{c}). \tag{2}$$

The last term of Eq. (1) specifies the NLC, which depends on the electric potential in the electrolyte, $\phi(x,z)$ [7,9]. The latter obeys to a very good approximation Laplace's equation (x and z are coordinates parallel and perpendicular to the electrode, respectively, and $z = \mathrm{WE}$ is the plane of the WE; σ is the dimensionless conductivity). The dependence of Eq. (1) on β makes explicit that the distance between WE and CE controls the NLC. This can also be seen by writing this term as an integral over a coupling function, $H_\beta(|x - x'|)$, as discussed in [10].

$$-\frac{\sigma}{\beta}(\partial_z \phi + \phi)|_{z=\mathrm{WE}} = \sigma \int_{\mathrm{WE}} H_\beta(|x-x'|) \times [\phi_{\mathrm{DL}}(x') - \phi_{\mathrm{DL}}(x)]dx'. \tag{3}$$

Through this approach, the migration coupling does not depend on $\phi(x,z)$, and therefore Eq. (1) is mathematically closed. For a 1D ring WE, we have [10]

$$H_\beta(|x-x'|) = \frac{\pi}{4\beta^2 \sinh^2(\frac{\pi(x-x')}{2\beta})} + \frac{\delta(|x-x'|)}{\beta}. \tag{4}$$

This function is represented for different β values in the inset of Fig. 1. Its Fourier transform is

$$H_{\beta}^{(q)} = -q\coth(q\beta) + \frac{1}{\beta}. \tag{5}$$

In the limit $\beta \longrightarrow 0$, the NLC becomes local (diffusion-like, $\sim q^2$) with "diffusion coefficient" $\sigma\beta/3$. In the limit $\beta \longrightarrow \infty$, Eq. (5) is, however, linear in q.

Let us now concentrate on the dynamics described by Eqs. (1) and (2). We define a vector $\mathbf{X}$ with ϕ_{DL} in its first entry and the concentrations of chemical species in the others. We denote the homogeneous dynamics by $F(\mathbf{X}, \mu)$ where μ is a control parameter. The NLC term now correlates $\mathbf{X}$ in space, and Eqs. (1) and (2) read

$$\partial_t \mathbf{X} = F(\mathbf{X}, \mu) + K \int_{\mathrm{WE}} H_{\beta}(|x - x'|)[\mathbf{X}(x') - \mathbf{X}(x)]dx' \tag{6}$$

where K is a matrix with $K_{11} = \sigma$ and all other elements are zero. We expand this dynamics in the vicinity of the steady state $\mathbf{X}^0$ in terms of the deviation $\mathbf{u} \equiv \mathbf{X} - \mathbf{X}^0$

$$\partial_t \mathbf{u} = L\mathbf{u} + K \int_{\mathrm{WE}} H_{\beta}(|x - x'|)[\mathbf{u}(x') - \mathbf{u}(x)]dx' + M\mathbf{u}\mathbf{u} + N\mathbf{u}\mathbf{u}\mathbf{u} + \ldots \tag{7}$$

where $L_{ij} = \frac{\partial F_i(\mathbf{X}^0)}{\partial X_j^0}$, $(M\mathbf{u}\mathbf{u})_i = \sum_{j,k} \frac{1}{2!} \frac{\partial^2 F_i(\mathbf{X}^0)}{\partial X_j^0 \partial X_k^0} u_j u_k$, and $(N\mathbf{u}\mathbf{u}\mathbf{u})_i = \sum_{j,k,l} \frac{1}{3!} \frac{\partial^3 F_i(\mathbf{X}^0)}{\partial X_j^0 \partial X_k^0 \partial X_l^0} u_j u_k u_l$. We focus on the dynamics close to a SHB in which a pair of complex conjugated eigenvalues crosses the imaginary axis ($\mu = 0$). For small μ, the critical eigenvalue λ_c becomes $\lambda_c \approx \lambda_0 + \mu\lambda_1$ and the Jacobian $L \approx L_0 + \mu L_1$ so that we have $L_j\mathbf{U} = \lambda_j\mathbf{U}$, $L_j\bar{\mathbf{U}} = \bar{\lambda}_j\bar{\mathbf{U}}$ ($j = 0, 1$), $\lambda_0 \equiv i\omega_0 = \mathbf{U}^* L_0 \mathbf{U}$, $\lambda_1 \equiv \gamma_1 + i\omega_1 = \mathbf{U}^* L_1 \mathbf{U}$, where $\mathbf{U}$ and $\mathbf{U}^*$ ($\mathbf{U}\mathbf{U}^* = 1$) are right and left eigenvectors, respectively, and the bar denotes complex conjugation. In a spatially extended system, the relevant eigenvalues governing the dynamics close to criticality are thus contained in a circle centered in the critical eigenvalue with radius proportional to $|\mu|$. We define the small parameter ε through $\chi\varepsilon^2 \equiv \mu$ where $\chi \equiv \mathrm{sgn}\mu$. Close to criticality, $\mathbf{u}$, L, M, and N, can be expanded in powers of ε as $\mathbf{u} = \sum_{k=1}^{\infty} \varepsilon^k \mathbf{u}_k$, $L = \sum_{k=0}^{\infty} \chi^k \varepsilon^{2k} L_k$, $M = \sum_{k=0}^{\infty} \chi^k \varepsilon^{2k} M_k$, $N = \sum_{k=0}^{\infty} \chi^k \varepsilon^{2k} N_k$. The dependence of λ_c on μ to first order suggests the introduction of an additional "slow" time variable $\tau = \varepsilon^2 t$ and, hence, $\partial_t \longrightarrow \partial_t + \varepsilon^2 \partial_\tau$. For nonvanishing β, the dispersion relationship of the NLC Eq. (5) depends to dominant order linearly in $q \equiv 2\pi n/L$ and $1/\beta$; i.e., it is proportional to the inverse of the characteristic length of the system. This contrasts with the spatial coupling caused by diffusion in reaction-diffusion systems, which in Fourier space depends on the squared inverse of the system length [1]. The NLC yields branches of eigenvalues separated by a distance of order σL^{-1} and only the ones within a circle of radius $|\mu|$ are relevant to the dynamics. Therefore, we scale space and coupling range, respectively, as $s = |\mu|x = \varepsilon^2 x$ and $\tilde{\beta} = |\mu|\beta = \varepsilon^2\beta$. Then, the coupling function Eq. (4) transforms as $H_{\beta}(|x - x'|) \longrightarrow \varepsilon^4 H_{\tilde{\beta}}(|s - s'|)$. The spatial integral of the coupling function contributes with ε^2 indicating that the nonlocal coupling is weak. This indeed makes possible the application of center-manifold theory [4]. By replacing all the above ε-dependent quantities in Eq. (7) and by equating terms with equal powers of ε, we obtain

$$(\partial_t - L_0)\mathbf{u}_k = \mathbf{B}_k \qquad (k = 1, \ldots, \infty) \tag{8}$$

where, to third order in ε, we have

$$\mathbf{B}_1 = 0 \qquad \mathbf{B}_2 = M_0\mathbf{u}_1\mathbf{u}_1 \tag{9}$$

$$\mathbf{B}_3 = -(\partial_\tau - \chi L_1)\mathbf{u}_1 + 2M_0\mathbf{u}_1\mathbf{u}_2 + N_0\mathbf{u}_1\mathbf{u}_1\mathbf{u}_1 + K \int_{\mathrm{WE}} H_{\tilde{\beta}}(|s - s'|)[\mathbf{u}_1(s') - \mathbf{u}_1(s)]ds' \tag{10}$$

the NLC entering at third order. If we write $\mathbf{B}_k(t, \tau, s) = \sum_{l=-\infty}^{\infty} \mathbf{B}_k^{(l)}(\tau, s)e^{il\omega_0 t}$, the linear Eqs. (8) satisfy a solvability condition for any k

$$\mathbf{U}^* \cdot \mathbf{B}_k^{(1)}(\tau, s) = 0 \tag{11}$$

which allows us to calculate the u_k's iteratively. The solutions for $\mathbf{u}_1$ and $\mathbf{u}_2$ follow then from Eqs. (8) and (9) as $\mathbf{u}_1 = W\mathbf{U}e^{i\omega_0 t} + \bar{W}\bar{\mathbf{U}}e^{-i\omega_0 t}$ and $\mathbf{u}_2 = -(L_0 - 2i\omega_0)^{-1} M_0\mathbf{U}\mathbf{U}(W^2 e^{2i\omega_0 t} + \bar{W}^2 e^{-2i\omega_0 t}) - 2L_0^{-1} M_0 \mathbf{U}\bar{\mathbf{U}}|W|^2$. By replacing these expressions in (10) and by using Eq. (11) for $k = 3$, we obtain

$$\partial_\tau W = \chi\lambda_1 W - g|W|^2 W + \tilde{K} \int_{\mathrm{WE}} H_{\tilde{\beta}}(|s - s'|) \times [W(s') - W(s)]ds' \tag{12}$$

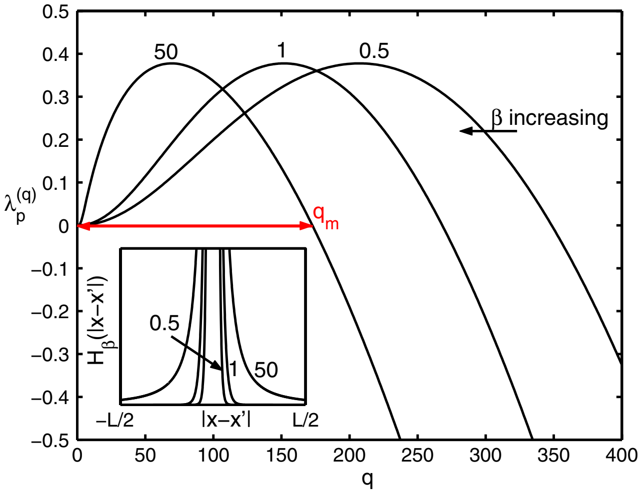

FIG. 1 (color online). Dispersion curves obtained from Eq. (14) for the values of β indicated in the graph, $c_1 = -1.03$, $c_2 = 2.68$. Inset: H_β calculated from Eq. (4) for $L = 20$.

where $\tilde{K} = \tilde{K}' + i\tilde{K}'' \equiv \mathbf{U}^* K \mathbf{U}$ and $g \equiv g' + ig'' = 4\mathbf{U}^* M_0[\mathbf{U}L_0^{-1}M_0\mathbf{U}\bar{\mathbf{U}} + \bar{\mathbf{U}}(L_0 - 2i\omega_0)^{-1}M_0\mathbf{U}\mathbf{U}] - 3\mathbf{U}^* N_0 \mathbf{U}\mathbf{U}\bar{\mathbf{U}}$ ($g' > 0$ at a SHB). By introducing scale transformations: $\tau \rightarrow \gamma_1^{-1}\tau$, $s \rightarrow \tilde{K}' s/\gamma_1$, $\tilde{\beta} \rightarrow \tilde{K}'\tilde{\beta}/\gamma_1$, $W \rightarrow \sqrt{\gamma_1/|g'|}\exp(i\omega_1\tau/\gamma_1)W$, and writing x, t, and β instead of s, τ, and $\tilde{\beta}$, we arrive at the NCGLE

$$\partial_t W = W - (1 + ic_2)|W|^2 W + (1 + ic_1) \times \int_{\mathrm{WE}} H_\beta(|x - x'|)[W(x') - W(x)]dx' \quad (13)$$

where $c_1 = \tilde{K}''/\tilde{K}'$, $c_2 = g''/g'$. Compared to the CGLE, the NCGLE depends on the additional parameter β that controls the range of the coupling. The homogeneous dynamics of electrochemical systems also depends on β through the parameter $\sigma_c = \sigma/\beta$ [9]. Experimentally, adjusting σ to keep σ_c constant allows the effect of β to be studied without changing the values of c_1 and c_2.

We have performed the stability analysis of the uniform oscillation with the NCGLE. The eigenvalue spectrum for phase-like fluctuations has the form

$$\lambda_p^{(q)} = -(1 - H_\beta^{(q)})\left\{1 - \sqrt{1 - \frac{H_\beta^{(q)}[(1 + c_1^2)H_\beta^{(q)} - 2\alpha]}{(1 - H_\beta^{(q)})^2}}\right\} \quad (14)$$

where $H_\beta^{(q)}$ is given by Eq. (5) and $\alpha \equiv 1 + c_1c_2$ (see supporting material [13]). To have an instability, $\lambda_p^{(q)} > 0$ and, therefore (since $H_\beta^{(q)} < 0$ for $q > 0$), we have $\alpha < 0$. α also controls the stability of the uniform solution in the CGLE with $\alpha = 0$ yielding the so-called Benjamin-Feir (BF) line in the $c_1 - c_2$ plane. In the case of the NCGLE, the dispersion relation depends also on β. Its effect on the spectrum can be seen in Fig. 1 for constant c_1 and c_2. When $\alpha < 0$, we enter in the phase turbulent regime, and any q lower than a wave number q_m given by $q_m \coth(q_m\beta) - \frac{1}{\beta} = \frac{2|\alpha|}{1+c_1^2}$ will destabilize the uniform oscillation. For small β, $q_m \coth(q_m\beta) - \frac{1}{\beta} \approx \beta q_m^2/3$ and therefore $q_m \approx \sqrt{\frac{6|\alpha|}{\beta(1+c_1^2)}}$. With increasing β, q_m decreases as $\sim\beta^{-1/2}$, and the band of unstable wave numbers (the interval $q \in [0, q_m]$) is compressed (see Fig. 1). The spatiotemporal structures have then larger characteristic lengths. For very high β, we have $q_m \coth(q_m\beta) - \frac{1}{\beta} \approx q_m$, and $q_m \approx \frac{2|\alpha|}{1+c_1^2}$ no longer depends on β (the NLC saturates). Note that, as clear from the inset in Fig. 1, the coupling function can have a global contribution, in which case only a few wave numbers are unstable. We have simulated the NCGLE by using a pseudospectral method with 512 Fourier modes, periodic boundary conditions, and an exponential time stepping algorithm [14]. The spatiotemporal evolutions of the modulus of the amplitude $|W|$ for two different β values are shown in Fig. 2. They confirm the conclusion from the above stability analysis: For larger β, the spatial structures are larger and the density of space-time defects is lower. Each defect is enclosed in a dark region of Fig. 2 where $|W|$ is low. These results are fully consistent with very recent experimental findings in which electrochemical turbulence was reported [8], the density of defects found to decrease with increasing β. When the NLC has a global contribution, turbulence can even be suppressed giving rise to spatially coherent structures. Several initial conditions were considered (a localized pulse in Fig. 2) and yielded similar asymptotic solutions.

We now calculate the coefficients c_1 and c_2 of the NCGLE, Eq. (13) from the dynamics of a N-type negative differential resistance (N-NDR) electrochemical oscillator [11] at the SHB. This two-variable N-NDR model was considered, for example, for the reduction of IO_4^- on an Au electrode. It is given by Eqs. (1) and (2) with [11]

$$f(\phi_{\mathrm{DL}}, c) = -k(\phi_{\mathrm{DL}}, c) + \sigma_c(U - \phi_{\mathrm{DL}}) \quad (15)$$

$$g(\phi_{\mathrm{DL}}, c) = [-k(\phi_{\mathrm{DL}}, c) + 1 - c]\epsilon. \quad (16)$$

Here, $\sigma_c \equiv \sigma/\beta$, $\epsilon = 10^{-4}$, and $k(\phi_{\mathrm{DL}}, c) = 7.293 \times 10^{-5}c(\phi_{\mathrm{DL}}^3 - 472.5\phi_{\mathrm{DL}}^2 + 55932\phi_{\mathrm{DL}})$. All quantities required to evaluate c_1 and c_2 are given in the supporting information [13]. In Fig. 3, we show the SHB curve in the $U - \sigma_c$ parameter plane. Since instabilities of the homogeneous steady state with nontrivial wave numbers are not possible in N-NDR systems [7], c_1 and c_2 can be calculated from the steady states at the SHB. The resulting curve is shown in Fig. 4. We find a parameter range in which the system is in the turbulent regime. At low applied voltage U, the uniform oscillation is stable. As U is increased, the $\alpha = 0$ line is crossed, and the instability develops. The inset in Fig. 4 shows that a further increase in U pushes the

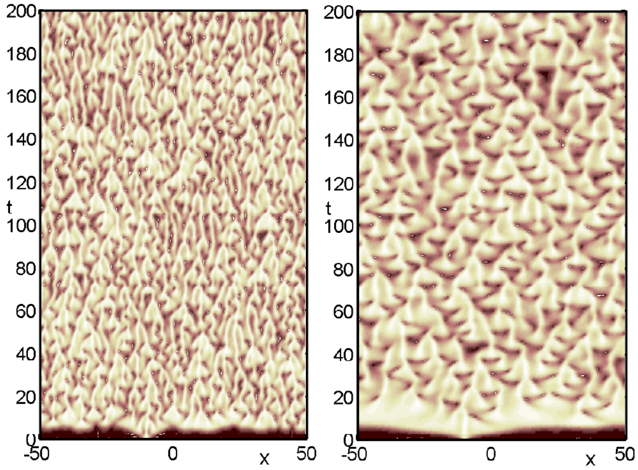

FIG. 2 (color online). Spatiotemporal evolution of the modulus of the amplitude $|W|$ for $c_1 = -1.03$, $c_2 = 2.68$, $L = 100$, and $\beta = 1$ (left) and 50 (right). Low $|W|$: dark.

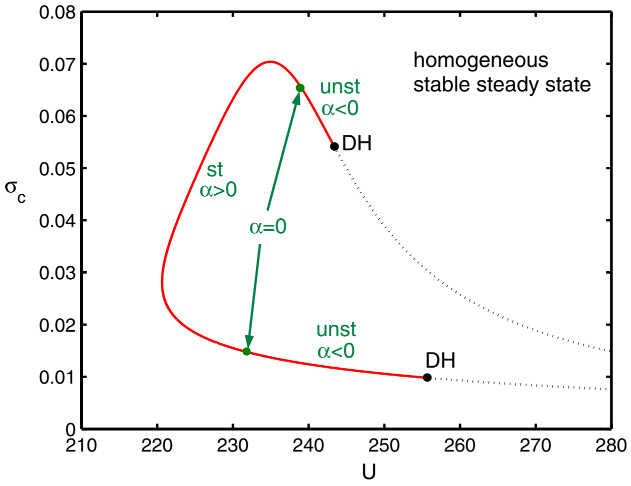

FIG. 3 (color online). Hopf curve for the N-NDR oscillator in the σ_c vs U plane (continuous line: SHB; dotted line: subcritical Hopf; DH: degenerate Hopf point). Uniform oscillations are unstable between the $\alpha = 0$ and the DH points. Beyond the DH, the Hopf bifurcation is subcritical and the analysis is not applicable.

system deeper into the unstable region, the defect turbulence becoming stronger. These results are fully consistent with the experiments in which the density of defects was found to increase with U [8]. U plays a crucial role in driving the system far from equilibrium, and its increased value can be generally conjectured to lead to more dissipative turbulent states.

In summary, we have rigorously derived the NCGLE valid for electrochemical oscillators with migration NLC. This equation extends the validity range of the CGLE to synchronizing NLC as found in these oscillators. The effect of the NLC has been elucidated by means of the stability analysis of the uniform oscillation. We found that a larger coupling range leads to a lower density of space-time defects and a larger characteristic length of the spatiotemporal structures. The dynamics of a N-NDR electrochemical oscillator has been also mapped onto the NCGLE, and we have shown that this system exhibits electrochemical turbulence in wide parameter ranges. All results found for this system shed light on very recent experimental results [8] in which transitions from limit-cycle oscillations to electrochemical turbulence were reported.

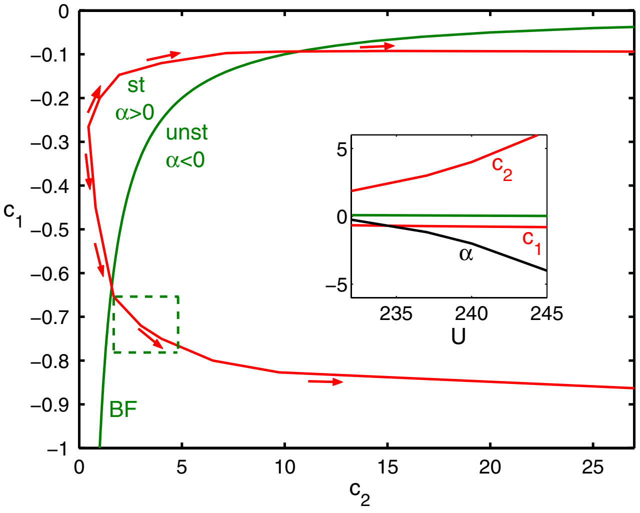

FIG. 4 (color online). Values for c_1 and c_2 for the N-NDR dynamics on the SHB shown in Fig. 3. Shown also is the $\alpha = 0$ (BF) line. Inset: c_1, c_2 and α vs U within the dashed box. Arrows indicate increasing U.

Fruitful discussions with R. Hölzel and financial support from the European Union (project DYNAMO, Contract No. 028669) and the excellence cluster Nanosystems Initiative Munich are gratefully acknowledged.

---

[*] vmorales@ph.tum.de

[†] krischer@ph.tum.de

[1] Y. Kuramoto, *Chemical Oscillations, Waves and Turbulence*, Springer Series in Synergetics (Springer, Berlin, 1984).
[2] I. S. Aranson and L. Kramer, Rev. Mod. Phys. **74**, 99 (2002); M. C. Cross and P. C. Hohenberg, Rev. Mod. Phys. **65**, 851 (1993).
[3] Y. Kuramoto, Prog. Theor. Phys. **94**, 321 (1995).
[4] D. Tanaka and Y. Kuramoto, Phys. Rev. E **68**, 026219 (2003).
[5] Y. Kuramoto, D. Battogtokh, and H. Nakao, Phys. Rev. Lett. **81**, 3543 (1998).
[6] D. M. Abrams and S. H. Strogatz, Phys. Rev. Lett. **93**, 174102 (2004).
[7] K. Krischer, in *Advances in Electrochemical Sciences and Engineering*, edited by D. M. Kolb and R. C. Alkire (Wiley-VCH, Weinheim, 2003), p. 89.
[8] H. Varela, C. Beta, A. Bonnefont, and K. Krischer, Phys. Rev. Lett. **94**, 174104 (2005).
[9] N. Mazouz, G. Flätgen, and K. Krischer, Phys. Rev. E **55**, 2260 (1997); F. Plenge, H. Varela, and K. Krischer, Phys. Rev. Lett. **94**, 198301 (2005).
[10] J. Christoph, Ph.D. thesis, Free University, Berlin, 1999; J. Christoph *et al.*, J. Chem. Phys. **110**, 8614 (1999).
[11] N. Mazouz *et al.*, J. Phys. Chem. B **101**, 2403 (1997); M. T. M. Koper and J. H. Sluyters, J. Electroanal. Chem. **303**, 73 (1991); M. T. M. Koper, Electrochim. Acta **37**, 1771 (1992); F. Plenge, Y.-J. Li, and K. Krischer, J. Phys. Chem. B **108**, 14255 (2004).
[12] S. Fukushima *et al.*, Electrochem. Comm. **7**, 411(2005).
[13] See EPAPS Document No. E-PRLTAO-100-044805 for supporting material. For more information on EPAPS, see http://www.aip.org/pubservs/epaps.html.
[14] S. M. Cox and P. C. Matthews, J. Comput. Phys. **176**, 430 (2002).